Modeling and optimization of bioreactor processes

José Pinto, João Antunes, João Ramos, Rafael S. Costa and Rui Oliveira*

LAQV-REQUIMTE, Department of Chemistry, FCTNOVA Science and Technology School, Universidade NOVA de Lisboa, Campus Caparica P-2829-516 Caparica, Portugal

*Corresponding author

Tel.: +351 212 948 356

Email: rmo@fct.unl.pt

Abstract

This chapter focuses on the topic of mathematical modeling of bioreactors, particularly dynamic modeling for measurement, modeling, monitoring and control applications. The first part of the chapter overviews mechanistic modeling across different scales, covering the concepts of structured/unstructured, segregated/unsegregated and genome-scale modeling. The second part of the chapter covers machine learning methods for supervised, unsupervised and reinforced learning in a bioprocessing context, with emphasis on building supervised bioreactor models that improve with process experience. Knowledge abstraction in the machine learning world is hardly compatible with the vast wealth of engineering and scientific knowledge accumulated over decades in the form of mechanistic models. The opportunities to develop hybrid mechanistic/machine learning models for bioreactors in the context of Industry 4.0 are finally highlighted. The vision is that machine learning should augment mechanistic bioreactor models rather than replace them. Several case studies are presented to illustrate the presented methods.

Keywords

Bioreactors, Mechanistic modeling, Machine learning, Hybrid modeling, Dynamic optimization

1. Introduction

Mathematical modeling is in its essence the translation of prior knowledge regarding the system at study into a compact mathematical representation. The translation of knowledge into a mathematical construct can be performed in many different ways, resorting to many different mathematical formalisms. This chapter focuses on a particular class of bioreactor dynamic models for Measurement, Modeling, Monitoring and Control (M3C) applications (Mandenius, 2004, Carrondo et al., 2012). Bioreactor dynamic models are essential tools to speed-up bioprocess development or for the control of large-scale production bioreactors. The aim of such models is to establish a quantitative cause-effect relationship between control degrees of freedom, state variables, measured variables, and a profit function, which is dynamic in nature. Such models are used for off-line simulation and optimization (the open-loop dynamic optimization problem), for on-line state and/or parameters estimation, for model predictive control, among many other applications. Recently, bioreactor dynamic models are being considered for the implementation of digital twins in the context of Industry 4.0 (Nargund and Mauch, 2019, McLamore et al, 2020, Moser et al., 2020, Jens et al, 2020).

Bioreactors are complex multi-scale processes that are very challenging to model (Fig. 1). For dynamic modeling of stirred tank bioreactors, homogeneity of the macroscopic scale is normally assumed. In scale-up problems, the understanding of the macroscopic heterogeneity becomes essential, for which the development of computational fluid dynamics models becomes a major challenge (not covered in this chapter). Cell cultures are in reality comprised of heterogeneous mixtures of cells that differ with regard to size, mass and intracellular concentrations of proteins, DNA and other chemical constituents. In many problems, population heterogeneity is an important factor to consider thereby substantially increasing the complexity of the model (Ataai and Shuler 1985; Domach

and Shuler 1984; Henson 2003a; Sidoli et al. 2004). The intracellular processes comprehend thousands of metabolic reactions and many more regulatory processes involving genes, RNAs, proteins and metabolites. In the last two decades, systems biology has led to an explosion of knowledge regarding intracellular processes, that can now be integrated in bioreactor models. In many bioreactor dynamic modeling problems, there is no need to consider all the scales with high level of detail. In cases when the product quality attributes are expressed at the molecular level (e.g. Glycosylation features of a biologic), all the scales potentially play a role, with the complexity of the model dramatically exploding.

Figure 1. The multiscale nature of a bioreactor system

There are currently two apparently conflicting approaches to address such complex bioreactor modeling problems (Baker et al, 2018): mechanistic modeling and data-based/machine learning. From one side, mechanistic modeling based on first Principles of physics, chemistry and biology has been the classical approach to develop bioreactor models. First Principles include the conservation laws of mass, energy and momentum, which may be stated for a bioreactor *ab initio* without the need of experimental evidence. Mechanistic models are frequently complemented with phenomenological and/or semi-empirical models to describe less defined parts of the process, for which prior mechanistic knowledge is still missing.

The other emerging vision is that of machine learning leveraged on high throughput data sets across different scales. Technological advances in bioprocesses research have pushed high-throughput instruments, with increasingly accurate data being collected (particularly proteomics, metabolomics, transcriptomics, and genomics data) (Palsson.B.O. 2002). With industry 4.0 enactment, such measurement devices will widespread and deliver

large-scale collections of datasets from heterogeneous sources, called in computational science as “big data” (Cook et al. 2018). Significant effort has been put into ensuring the scalability of computational tools for the collection of these massive bioprocess data, but analysis and integration remains a challenge (Qin et al. 2015). The availability of data has been one of the most notable advances in predictive modeling. With this background, the deployment of machine learning in a bioprocessing context will likely grow in the future, including the application for bioreactor modeling, optimization and control (the M3C challenge). Particularly, machine learning offers the possibility of modeling complex bioreactor data sets across multiple scales, with the ability to identify patterns and learn and improve through time, thereby realizing Industry 4.0 vision (Jordan and Mitchell 2015). In parallel to the emergence of machine learning, a new movement towards hybrid approaches that combine mechanistic modeling with machine learning is getting momentum (Galvanauskas et al., 2004, Oliveira, 2004, von Stosch et al., 2014). The vision is that machine learning should be used to augment mechanistic models rather than to replace them. Hybrid modeling combines the power of mechanistic understanding and predictive modeling thus particularly attractive for tackling complex bioreactor modeling problems.

The first part of this chapter overviews the key mechanistic modeling concepts for a bioreactor system emphasizing the multi-scale nature and the many challenges yet to overcome. In particular, the reduction and integration of genome-scale models with bioreactor models is discussed. The second part of the chapter covers machine learning methods for supervised, unsupervised and reinforced learning in a bioprocessing context, with emphasis on building supervised bioreactor models that improve with process experience. It finalizes with an overview of hybrid mechanistic/machine learning models

for bioreactors in the context of Industry 4.0. Several case studies are presented to illustrate the presented methods.

2. The traditional approach: bioreactor mechanistic models

A bioreactor mathematical model may be expressed in different ways depending on the objective of the model. This chapter will address a particular class of dynamic models for perfectly mixed bioreactors expressed by the following general state-space representation:

$$\frac{dx}{dt} = f(x(t), u(t), \theta_x, t); \quad x(t_0) = x_0 \tag{1a}$$

$$y = h\big(x(t), \theta_y\big) \tag{1b}$$

with x(t) the state vector, $u(t)$ the control vector, $y(t)$ the vector of measured variables, θ_x and θ_y the parameters vector of the state –space and measurement models respectively, and *t* the dependent variable time. Eq. (1a) is the state-space model while Eq. (1b) is the measurement model. The functions $f(\cdot)$ and $h(\cdot)$ are typically complex and nonlinear, which render bioreactors rather complex dynamical systems, which are difficult to identify and to control. The system of Eqs. (1a,b) may be shaped in many different ways depending on the level of detail of the knowledge available, as shown in the proceeding sections.

2.1 Macroscopic material balances

Macroscopic bioreactor dynamics may be established *ab initio* by the material balance equations of the key extracellular compounds that intervene in the reaction mechanism. These material balances are expressed by systems of ordinary differential equations (ODEs), which take the following general state-space form (Bastin and Dochain, 1990):

$$\frac{dc}{dt} = r - Dc + Dc_{in} + q \quad (2a)$$

with c a vector of n concentrations of extracellular compounds (the state vector), r a vector of n volumetric reaction rates, $D = F/V$ the dilution rate (F is the volumetric feeding rate into the reactor and V the liquid volume inside the reactor), c_{in} is a vector of n concentrations of extracellular compounds in the inlet stream, and q a vector of n volumetric exchange rates from the gas to the liquid phase, which apply to gases (e.g. O_2, CO_2, H_2, CH_4, etc…) and extracellular volatile compounds which are typically low molecular weight metabolites resulting from the central carbon metabolism (e.g., ethanol, methanol, etc…). Eq. (2a) must be complemented with the general mass balance equation. If the specific mass of the inlet stream is not significantly different than that of the liquid inside the bioreactor, the following simplified general mass balance applies:

$$\frac{dV}{dt} = DV \quad (2b)$$

Eqs (2a,b) are generic for perfectly mixed bioreactors irrespective of the operation mode. In batch reactors, system (2a,b) holds with $D = 0$. Fed-batch bioreactors are expressed by system (2a,b) as is. A CSTR in transient operation is modeled with Eq (2a) plus $\frac{dV}{dt} = F - F = 0$ (volume is constant). A CSTR in steady state is modeled with system (2a,b) by making all derivatives equal null, i.e $0 = r - Dc + Dc_{in} + q$ and $\frac{dV}{dt} = 0$.

The system (2a,b) must be completed with defining kinetic Eqs. for the gas-liquid volumetric transfer rate, q, and for the volumetric reaction term, r. Gas-liquid mass transfer models are well covered in reference text books (e.g. Bailey and Ollis, 1986, Blanch and Clarck, 1996) and will not be covered here. The critical challenge in bioreactor engineering is the modeling of the reaction kinetics, which will be further covered below.

2.2 Unstructured growth models

The simplest approach to define a bioreactor model is by considering the cells all equal (unsegregated) and without intracellular structure (unstructured). These assumptions give rise to unstructured growth models, which were the prevailing type of models until the early 00s. The extracellular compounds are considered as biochemical species that intervene in a simplified bio-reaction mechanism, with biomass the catalyst of such bio-reactions. As illustrative example, a simple bio-reaction mechanism whereby biomass (X) grows on a limiting substrate (S) resulting in the formation of itself (X) and product (P), may be expressed as:

$$y_{\frac{S}{X}}\, S \xrightarrow{\mu} 1\, X + y_{P/X} P \tag{3a}$$

$$y_{S/P}\, S \xrightarrow{m_P} 1\, P \tag{3b}$$

$$S \xrightarrow{m_S} \emptyset \tag{3c}$$

$$X \xrightarrow{k_d} \emptyset \tag{3d}$$

The first reaction (3a) represents cell growth with concomitant formation of product (P) (cell growth associated product synthesis). The reaction (3b) represents cell growth dissociated product formation. The reaction (3c) represents the substrate metabolized for cellular maintenance. The reaction (3d) represents biomass death. The yields $y_{i/j}$ are stoichiometric coefficients typically defined on a mass basis due to the undefined nature of some biochemical species, particularly biomass. The specific growth rate, μ, is normally defined by the Monod model (Monod, 1949) to express growth limitation by susbstrate S:

$$\mu = \mu_{max} \frac{[S]}{K_S + [S]} \tag{4}$$

with μ_{max} the maximum cell growth rate, $[S]$ is the substrate concentration, and K_S the Monod constant. The Monod model is inspired in the irreversible Michaelis-Menten enzyme kinetics but is of empirical nature. To express growth inhibition by high substrate concentrations, the Andrews model (Andrews, 1968) is a common choice,

$$\mu = \mu_{max} \frac{[S]}{K_S + [S] + \frac{[S]^2}{K_{I,s}}} \quad (5),$$

with $K_{I,s}$ the substrate inhibition constant. The Andrews model is inspired in the Hans and Levenspiele acid-base equilibrium model for enzyme kinetics. Hans and Levenspiel (1988) have extended the Monod model by considering the effect of $i = 1, \ldots, h$ inhibitors of cell growth,

$$\mu = \mu_{max} \prod_{i=1}^{h} \left(1 - \frac{[I_i]}{[I_i^*]}\right)^{n_i} \left(\frac{[S]}{[S] + K_S \prod_{i=1}^{h} \left(1 - \frac{[I_i]}{[I_i^*]}\right)^{m_i}} \right) \quad (6),$$

with $[I_i]$ the concentration of inhibitor I_i. This model assumes the existence of a critical inhibitor concentration $[I_i^*]$ above which cells cannot grow, and that the constants of the Monod equation are functions of this limiting inhibitor concentration. The n_i, m_i are additional kinetic parameters that need to be estimated from data. The Monod model may also be extended to express the limitation of multiple n_s substrates and the inhibition of multiple n_p products.

$$\mu = \mu_{max} \prod_{i=1}^{n_s} \frac{[S_i]}{K_{Si} + [S_i]} \prod_{i=1}^{n_P} \frac{K_{Pi}}{K_{Pi} + [P_i]} \quad (7)$$

The specific product synthesis rate, v_P, maybe expressed by the Luedeking-Piret equation (Luedeking and Piret, 1959)

$$v_P = y_{P/X}\mu + m_P \quad (8),$$

which considers a growth associated product synthesis term (Reaction 3a) and a growth dissociated term (Reaction 3b). These reaction kinetics and many other are simplified phenomenological models commonly referred to as Monod-type kinetics.

Linking with the macroscopic balance Eqs. (2a) needs the definition of the volumetric reaction rates, which for the case of unstructured growth models take the following general form

$$r = K\, v(c,u,\theta)\, X \tag{9}$$

with $K = \{y_{i/j}\}$ a $n \times m$ matrix of yield coefficients and $v(c,u,\theta)$ the vector of specific reaction rates. The yield coefficients in matrix K have been often observed dependent of the experimental conditions. This apparent time-varying nature of yield coefficients is explained by the lack of intracellular structure in the model. Metabolic pathway analysis of genome scale networks have highlighted the redundant nature of biochemical networks, characterized by millions of metabolic circuits between extracellular substrates and end products in prokaryotes and even more in eukaryote cells. The ability to dynamically adjust intracellular states explains the time-varying nature of yield coefficients and the lack of predictive power of purely macroscopic models. In many cases the consideration of intracellular structure becomes mandatory, which will be further covered in the next sections.

Box 1 illustrates a simple macroscopic model coupled with unstructured kinetics. This model describes the dynamics of 5 state variables in a fed-batch bioreactor for the cultivation of a recombinant yeast for the production of a heterologous protein (Park and Ramirez, 1988). The Park and Ramirez bioreactor model is considered a benchmark dynamic optimization problem that will be addressed in section 2.5.

Box 1: The Park and Ramirez bioreactor model (Park and Ramirez, 1988).

The Park Ramirez bioreactor models describes a fed-batch culture of the *Saccharomyces cerevisiae* SEY2102 expressing the heterologous protein SUC-s2. The model comprises 5 state variables: P_M - concentration of secreted SUC2-s2; P_T - concentration of total SUC2-s2; X - biomass concentration; S - glucose concentration; V – culture volume. The growth kinetics are unstructured with 3 rate equations: Φ – SUC2-s2 secretion rate; f_P – SUC2-s2 expression rate; μ – specific growth rate. The model equations are as follows.

Macroscopic material balances:

$$\frac{dP_M}{dt} = \Phi(P_T - P_M) - DP_M \quad (1.1)$$

$$\frac{dP_T}{dt} = f_P X - DP_T \quad (1.2)$$

$$\frac{dX}{dt} = \mu X - DX \quad (1.3)$$

$$\frac{dS}{dt} = -Y\mu X - DS + DS_{in} \quad (1.4)$$

$$\frac{dV}{dt} = DV \quad (1.5)$$

Unstructured kinetic rates:

$$\Phi = \frac{4.75\mu}{0.12+\mu} \quad (1.6)$$

$$f_P = \frac{S\, e^{-5S}}{0.1+S} \quad (1.7)$$

$$\mu = \frac{21.87S}{(S+0.4)(S+62.5)} \quad (1.8)$$

Concentrations of extracellular species (units g/L): $c = [P_M\ P_T\ X\ S]^T$

Concentrations in the inlet stream: $c_{in} = [0\ 0\ 0\ S_{in}]^T$

Volumetric reaction rates (units g/Lh) : $r = [\Phi(P_T - P_M),\ f_P X,\ \mu X,\ -Y\mu X\ ]^T$

Volumetric gas-liquid transfer rates (units g/Lh) : $q = [0,\ 0,\ 0,\ 0]^T$

Control degrees of freedom: F(t) with $D = F/V$

Initial conditions and other constants:

$P_M(t=0) = 0\ g/L,\quad P_T(t=0) = 0\ g/L,\quad X(t=0) = 1\ g/L,\quad S(t=0) = 5\ g/L,$
$V(t=0) = 1\ L, Y = 0.7 g/g, S_{in} = 20\ g/L$

Fifteen (15) cultivation runs were simulated with varying feeding rate, F, over time. The F time profile was designed by central composite design (CCD) with 3 factors, each factor

representing a constant feeding rate in a time interval of 5 hours (Fig. 2). A 16th run was simulated with the optimal feeding profile calculated by Park&Ramirez (1988). The optimal cultivation is signaled in Fig. 2 by the points with black edge color. These simulations served as synthetic dataset for modeling studies in the proceeding sections of this chapter. A Gaussian error was added with standard deviation of 0.1 for all variables except for substrate which was 0.25 g/L.

Figure 2. Simulation of 16 cultivation runs with the Park and Ramirez (1988) model eqs. (1.1-1.7). Numerical integration proceeded with a Runge-Kutta 4th/5th order solver. Small points refer to the simulation of 15 runs with 3 levels of constant feeding rate designed by central composite design with 3 factors, each factor representing a constant feeding rate in a 5-hour interval. The larger points represent the Park&Ramirez optimal control solution with maximal productivity of 32.4 g of secreted in the end of the culture.

2.3 Segregated growth models

Cell cultures are in reality comprised of heterogeneous mixtures of cells that differ with regard to size, mass and intracellular concentrations of proteins, DNA and other chemical constituents. To account for population heterogeneity, population material balance equations are applied to segregate groups of cells with identical properties. In a population balance based on cell number, the cells are differentiated in terms of a given set of properties, y. The distribution of cells in the population in relation to properties y is given by a distribution function $w(y,t)$, where $w(y,t)dy$ represents the number of cells per unit volume within the property interval $[y, y+dy]$ at time t. The total cell count is then given by:

$$w(t) = \int_{y_{min}}^{y_{max}} w(y,t)dy \qquad (10).$$

The distribution function $w(y,t)$ is obtained by solving the population balance equation (PBE), which for a homogeneous homogenous bioreactor without cell feeding, takes the following general form (Nielsen and Villadsen, 1994):

$$\frac{\partial w(y,t)}{\partial t} + \frac{\partial [r(y,t)w(y,t)]}{\partial y} = h(y,t) - Dw(y,t) \quad (11)$$

with $r(y,t)$ the rate of change of property y, and $h(y,t)$ the net rate of formation of cells with the property y due to cell division, and D the dilution rate in the bioreactor. The net rate of formation of cells with the property y due to cell division maybe further detailed by splitting into the rates of formation and disappearance of cells with property y,

$$h(y,t) = 2\int_{y_{min}}^{ymax}(y',t)p(y,y',t)w(y',t)dy' - (y,t)w(y,t) \quad (12),$$

with (y',t) the division rate of cells with property y', $p(y,y',t)$ the probability of a mother cell with property y' dividing into 2 daughter cells with property y.

The link with the macroscopic material balances requires a modification of Eq. (2a) to account for the influence of properties y in the specific reaction rates, v, as follows:

$$r = K\int_{y_{min}}^{y_{max}} v(c,y,u,\theta)\, w(y,t)dy \quad (13).$$

For simplicity, PBE are usually applied to a single property such as cell age (A. Hjortso and Nielsen 1995) or cell mass (Nishimura and Bailey 1981). Since it considers growth and division of single cells, this approach can be used to describe heterogeneity caused by extra and intracellular fluctuations (Delvigne et al. 2014). Many PBE models have been developed (Anderson et al. 1969; Fadda et al. 2012; Ganusov et al. 2000; Henson 2003a; Zhu et al. 2000) and several numerical methods were developed to reduce the computational hurdles for solving the resulting nonlinear integro-ordinary differential and integro-partial differential equations (Liu et al. 1997; Mantzaris et al. 2001; Pigou et al. 2017; Singh et al. 2020).

2.4 Intracellular structure

Structured models further consider intracellular compartments (cytosol, mitochondria, nucleus, etc…) and the concentrations of intracellular species (metabolites, proteins, RNA/DNA and other chemical constituents), which are involved in a very complex network of physio-chemical transformations. Under the assumption of well-mixed compartments, the dynamic material balance equations over intracellular species are generically stated as:

$$\frac{dz}{dt} = N^{\{z\}}v - \mu z \qquad (14)$$

with z a vector of concentrations of nz intracellular species, $N^{\{z\}}$ a $nz \times q$ stoichiometric matrix of intracellular reactions, v a vector of q specific reaction rates (including transport reactions across compartments), and μ the specific growth rate. The second term in the right-hand side of Eq (14) expresses the dilution of intracellular species due to the increase of cell mass. The reaction rates, v, are complex functions of extracellular concentrations, c, intracellular concentrations, z, input variables (such as T, pH, etc) and kinetic parameters, θ:

$$v = f(z, c, u, \theta) \qquad (15)$$

The development of structured models has been historically limited by the lack of knowledge of the very complex intracellular phenomena. With the emergence of systems biology in the early 00s, several GEnome-scale reconstructed Models (GEM) have been developed for industrially relevant cells such as *Escherichia coli* (Monk et al., 2013), *Saccharomyces cerevisiae* (Foster et al., 2003), *Pichia pastoris* (Sohn et al., 2010), CHO cells (Hefzi et al., 2016), HEK cells (Quek et al., 2014) and many other. This new generation of GEMs are now being considered for bioreactor dynamic modeling, control and optimization. Construction of large dynamic GEMs has been attempted in two ways

(Stanford et al., 2013): i) traditional kinetic modeling paradigm, or ii) dynamic flux balance analysis techniques (dynamic FBA). Dynamic FBA avoids the definition of the kinetic rate Eqs. (15) by dynamic optimization of a cellular objective function (Mahadevan et al., 2002). However, rigorous dynamic modeling requires the definition of the kinetic Eqs. (15). One advantage of GEMs is the association between genes, enzymes, reactions and respective catalytic mechanisms. For bi-molecular metabolic reactions the mechanistic Michaelis-Menten model generally applies (Cornish-Bowden, 1995). A large number of metabolic reactions involve more than 1 substrate or more than 1 product. For such reactions, Liebermeister et al. (2010) proposed a generalized form of the reversible Michaelis-Menten model called modular rate law, which is now popular for GEM (Box 2). Unfortunately, most of the reaction mechanisms in GEMs are unknown and approximations are required, such as generalized mass action (GMA), hill kinetics, lin-log kinetics (Visser and Heijnen, 2003), convenience kinetics (Liebermeister and Klipp, 2006) and power laws (Savageau, 1970) and their combinations (Costa et al. 2010). GMAs are simplistic approximations of the reaction mechanisms based on the principle that the reaction rate is proportional to the probability of collision of reactant molecules. GMAs have only 2 parameters and they can be automatically generated from the reaction stoichiometry, which have popularized them in GEM.

Box 2: Kinetic models used in genome-scale modeling (GEMs)

Modular rate law (*Liebermeister et al., 2010*)

Principle: enzyme mechanism where ns substrates, S_i, and np products, P_j, bind rapidly and in random order

$$g_1S_1 + \cdots + g_{ns}S_{ns}k- \leftrightarrow h_1P_1 + \cdots + h_{ns}P_{np}$$

$$v = [E]\frac{k^+\prod_i \frac{[S_i]}{K_M^{Si}} - k^-\prod_j \frac{[P_j]}{K_M^{Pj}}}{\prod_i\left(1+\frac{[S_i]}{K_M^{Si}}\right) + \prod_j\left(1+\frac{[P_j]}{K_M^{Pj}}\right) -} \quad (2.1)$$

Parameters:
k^+, k^-- forward and backward turnover constants; K_M^j- dissociation constant of species j (the same interpretation as in the Michaelis-Menten model); $[E]$: amount of enzyme

Hill kinetic model

*Principle***:** reaction mechanism

$pG + nR \leftrightarrow pGR_n$ (active gene)

pG: gene promotor
R: regulator molecule
pGR_n: gene-regulator complex

$$v = \frac{v_{max}[R]^n}{K_a^n+[R]^n} \text{ (activation)} \quad (2.2)$$

$$v = \frac{v_{max}K_a^n}{K_a^n+[R]^n} \text{ (repression)} \quad (2.3)$$

*Parameters***:**
v_{max} – maximum transcription rate; K_a- half saturation constant; n-cooperativity ($n < 1$: negative cooperativity; $n = 1$: no cooperativity; $n > 1$: positive cooperativity)

Generalized mass action (GMA) approximation

Principle: reaction rate is proportional to the probability of collision of reactant species

$$g_1S_1 + \cdots + g_{ns}S_{ns}k- \leftrightarrow h_1P_1 + \cdots + h_{ns}P_{ns}$$

$$v = k^+\prod_{i=1}^{ns} S_i^{gi} - k^-\prod_{i=1}^{np} P_i^{hi} \quad (2.4)$$

*Parameters***:**

k^+, k^-: forward and backward kinetic constant; g_i: stoichiometric coefficients associated with ns substrates; h_i: stoichiometric coefficients associated with np products

---

The link with the macroscopic material balances (Eq. 2a) is not explicit in Eq. (15). A subset of reactions in vector, v, is associated with transport processes across the cellular membrane for the exchange between intracellular and extracellular compartments. The net volumetric reaction rate of n extracellular species can then be calculated as,

$$r = X\, N^{\{c\}}\, v \tag{16}$$

with $N^{\{c\}}$ the $n \times q$ stoichiometric matrix associated with n extracellular compounds. Eq. (16) links with the macroscopic material balances (Eq. 2a), which may be rewritten as

$$\frac{dc}{dt} = X\, N^{\{c\}}\, v - Dc + q \tag{17}$$

Given the very large size of $N^{\{z\}}$, $N^{\{c\}}$ and v with thousands of species and reactions, it is critical reduce GEMs to the reactor operating conditions. As illustrative example, Quek et al. (2014) have adapted the RECON-2 model (Thiele et al., 2013) with 7440 reactions for the cultivation of HEK293 cells in a defined medium, with a significative reduction to 329 reactions.

2.5 Dynamic optimization

Once the bioreactor dynamic model Eqs. 1(a,b) are established with more or less detail, optimal control scenarios may be investigated by applied dynamic optimization methods. The objective is the determination of the optimal control variables (the vector $u(t)$ in

system (1a,b)) such as to maximize a given profit function. This dynamic optimization problem has been generically stated as follows (Banga et al., 2003):

Find *u(t)* to minimize (or maximize) a performance index *J*,

$$J = \psi\left(x\left(t_f\right), t_f\right) + \int_{t_0}^{t_f} \phi(x(t), u(t), t)dt \quad (18a)$$

subject to:

i) to dynamic (bioreactor dynamic model) constraints

$$\frac{dx}{dt} = f(x(t), u(t), t) \quad ; \quad x(t_0) = x_0 \quad (1a)$$

ii) equality and inequality algebraic constraints,

$$h\left(x(t), u(t)\right) = 0 \quad (18b)$$

$$g\left(x(t), u(t)\right) \leq 0 \quad (18c)$$

iii) upper and lower bounds constraints of the state and control variables

$$x^L \leq x(t) \leq x^U \quad (18d)$$

$$u^L \leq u(t) \leq u^U \quad (18e).$$

The performance index (J) function considers two terms. The function $\psi\left(x\left(t_f\right), t_f\right)$ represents the endpoint reward/cost term. The function $\phi(x(t), u(t), t)$ represents a time dependent reward/cost term. There are three main approaches to solve this dynamic optimization problem:

- *Indirect dynamic optimization* is based on the conversion of the original dynamic optimization problem into a two-point boundary value problem using the necessary conditions of Pontryagin (Bryson and Yu-Chi, 1975).
- *Direct dynamic optimization* transforms the original dynamic optimization problem into a non-linear programming (NLP) problem. With this approach there are two strategies regarding the parameterization of the NLP problem: control

vector parameterization (CVP), in which the only variables parameterized are the control variables, and complete parameterization (CP), where both the control and state variables are parameterized.

- *Dynamic Programming* (DP): was developed by Bellman (1959) and has various uses in a wide array of fields. In the domain of bioreactor optimization, it has been utilized in the form of Iterative Dynamic Programming (IDP) – Luus (1992).

Among the three approaches, the most popular for bioreactor dynamic optimization is the direct approach with control vector parameterization (CVP), maybe due to the ease of implementation, resorting to well-known numerical methods. These include Deterministic Global Optimization methods (mainly quasi-Newton and Sequential quadratic programming) and Stochastic global optimization methods (Simulated annealing (Kirkpatrick et al., 1983), Evolutionary algorithms (Holland (1975), Particle swarm optimization (Kennedy & Eberhart, 1995), Ant-colony optimization (Dorigo et al., 1996), and many others). Global optimization methods suffer from the problems of non-convexity and non-smoothness typical of bioreactor problems, as the computational cost scales quickly with the dimensionality of the problem and optimality is not guaranteed. Indeed, no algorithm can solve general global optimization problems with certainty in finite time. Moreover, without any prior known structure or assumption about the model, there is no definitive best method – Wolpert & Macready (1997). Box 3 illustrates the application dynamic optimization to the Park&Ramirez bioreactor model.

Box. 3 Dynamic optimization of the Park and Ramirez (1988) bioreactor

Different methods of dynamic optimization were applied to the Park and Ramirez (1988) bioreactor model (described in Box 1). The performance index function was the maximization of the endpoint secreted protein mass:

$$J = PM(tf)V(tf) \quad (3.1),$$

with $tf = 15$ cultivation hours. The feeding rate over time, $F(t)$, bounded between 0 and 2 l/h, was the single control degree of freedom. The piecewise constant parameterization method was adopted in all runs:

$$F(t) \approx F^k(t) = \xi_k, \quad t \in [\tau_{k-1}, \tau_k], \quad k = 1, \dots, p \quad (3.2),$$

with p the number of discretization steps and ξ_k the constant feeding rate at time interval $[\tau_{k-1}, \tau_k]$. The following methods were implemented and compared with the results published by Park and Ramirez (1988): *truncated newton conjugate* (Nocedal and Wright, 1999), *basin hopping* (Wales and Doye, 1997), *dual annealing* (Xiang *et al.*, 2013), *particle swarm optimization* (Kennedy and Eberhart, 1995), a simple *genetic algorithm* (Thomas Back, 2000), *differential evolution* (Storn and Price, 1997) and *iterative dynamic programming* (Luus, 1992). For the sake of comparability, each optimization algorithm was run 10 times with a maximum limit of 50000 function evaluations per run and $p = 10$ discretization intervals. The relative error to the Park and Ramirez (1988) solution ($J = PM(tf)V(tf) = 32.4\ g$) was saved and compared. The overall results are shown in Fig. (3B). The different algorithms were very efficient at solving this problem, with the final objective function varying between 31.3 - 32.2 g in all runs, thus quite close to the Park&Ramirez optimal solution of 32.4 g. Analyzing the cumulative percentage undersize (in relation to the Park and Ramirez solution), the best methods were the

differential evolution and *iterative dynamic programming*, which delivered practically the same final solution irrespective of the starting point. The least efficient methods were *basin hopping* and truncated newton conjugate. Fig. (3C-E) shows the dynamic profiles obtained by the most efficient method (*differential evolution*) with $p = 45$ discretization intervals.

Figure 3. Dynamic optimization for the Park and Ramirez (1988) bioreactor problem. A – Direct dynamic optimization with control vector parameterization schematic representation. B - Comparison of cumulative percentage undersize for different optimization methods run 10 times with a maximum limit of 50000 function evaluations with 10 discretization intervals. C – Optimal feeding profile and reactor volume obtained with the *differential evolution* method with 40 discretization intervals. D - Optimal biomass and substrate profiles obtained with the *differential evolution* method with 40 discretization intervals. E - Optimal total and secreted protein profiles obtained with the *differential evolution* method with 40 discretization intervals.

---

3. Bioreactor models for Industry 4.0

Industry 4.0 is now widely accepted as the next paradigm for production with the widespread of automation, data connectivity and machine learning (ML). ML is an essentially part of Industry 4.0 that allows systems and algorithms to automatically improve based on experience. In this section it is cover the key concepts and the challenges of machine learning and hybrid mechanistic/machine learning modeling.

3.1 Machine Learning for bioreactor problems

Machine learning (ML) explores the capability of computational algorithms to learn from previous large experimental data. In this context, ML employs a variety of algorithms to automate the process of data-driven models construction, which iteratively learn to predict and improve different process outcomes (Jordan and Mitchell 2015). Several ML algorithms have been developed and are currently available in open-source python packages like *scikitlearn* (Pedregosa et al. 2011). Here we focus on ML methods that are often used in bioreactor applications. The ML area can be divided in three main classes: supervised, unsupervised, and reinforcement learning (Breve and Pedronette 2016, Nian et al. 2020, Singh et al. 2016).

- ***Supervised learning****:* The supervised learning methods, such as regression (for continuous/numeric outcomes) and classification (for categoric outcomes) problems, are techniques where the task is to create a relation between a set of input/feature observations (u) and the corresponding real-valued outcome (y label) in a training dataset. Mathematically this relationship is described by:

  $$y = f(u|\theta) \quad (19)$$

  Where, $f(.)$ is the model and θ the parameters. The main goal is to optimize θ, in order to minimize the error between the model and the real values given in the training dataset (Alpaydin 2020). Fig. (4) depicts a typical workflow applied in supervised learning.

- **Unsupervised learning:** Unlike supervised learning, where the data is labeled with the desired outcome value (i.e. the output associated to an observation is known), in unsupervised algorithms (learning without supervision) no pre-existing labels are required (Larranaga et al. 2006). The goal of unsupervised machine learning is to detect patterns in highly complex/multivariate input data

(e.g. regions of images or search results). In other words, the basic idea is to group together similar instances using for instance the Euclidean distance. Examples of unsupervised learning techniques are K-means clustering (Yu et al. 2020) and dimensionality reduction (DR) (Butcher and Smith 2020) (more details in Box 4).

- **Reinforcement Learning:** A different paradigm regarding learning from experience is provided by reinforcement learning (RL) (Sutton and Barto 1998). RL is based on the relationship between an *agent* and the *environment*; the *agent* observes the state of the *environment* in order to take actions. For instance, in bioreactors the state observed by the agent could be the strains of microorganisms and the RL action taken by the agent control can be the concentration of substrate. The goal of a RL algorithm is to use evaluative feedback from the environment to estimate real values to update an internal policy that optimizes a desired target (Lee et al. 2018). RL can be viewed as a joint optimization problem between the policy/action and the data. Despite some challenges (e.g. satisfying operational constraints), RL can be very useful to address a wide range of chemical process control and bioprocess problems. Some examples include the nonlinear optimal control problems (Hoskins and Himmelblau 1992, Shin et al. 2019) and real-time optimization of bioreactors (Powell et al. 2020). More recently, RL has been also applied for the control of bioreactor systems (Ma et al. 2020).

In what follows, three of the commonly used supervised learning methods in bioreactor modeling are further detailed.

Figure 4. Workflow for typical supervised machine learning algorithms**.**

3.1.1 Artificial Neural Networks (ANNs)

Neural network computing is currently the most popular ML tool for supervised learning in different domains including bioreactor modeling and control. ANNs are computing systems inspired by biological neural networks, consisting of multiple interconnected processing units (called nodes) arranged in layers (Haykin, 2009). Each node is excited by the connecting nodes (typically from preceding layers) and computes an output signal that will excite other nodes in the network (typically in proceeding layers). The nodes of the first layer (input layer) receive external signals, which are propagated to the nodes of the intermediate layers (hidden layers) eventually exciting the output nodes (output layer) thereby forming the system outputs. Different ANN architectures with particular node activation functions (linear, sigmoidal, tangent hyperbolic, reLU, etc...) and topologies have been proposed for different applications (Krogh 2008).

Neural network applications for bioreactor modeling and control have first caught attention in the early 90s (e.g. Dimassimo et al. 1992, Dochain, et al., 1992, Joseph and Hanratty, 1993, Baughman and Liu, 1994). This surge was motivated by the publication of the error back-propagation algorithm for efficient neural network training (Rumelhart et al. 1986), which boosted neural network applications in different domains. After a long period of skepticism they are now resurging by the new developments in deep neural network topologies and deep learning algorithms (Larochelle et al. 2009), particularly the ADAM algorithm (Kingma and Ba, 2017).

Given the non-linear character of bioreactor dynamics, the network topology mostly used is by far the Multilayer Perceptron Network (MLP). Particularly, a simple 3-layered MLP has been the topology of choice for now-linear regression problems in the bioreactor modeling domain. A 3-layered MLP for nonlinear regression problems consists of a linear

input layer, a single hidden layer with tangent hyperbolic nodes and an output linear layer. Mathematically, a MLP is simply stated by the following function,

$$y = w_2\, tanh(w_1 u + b_1) + b_2 \quad (20),$$

with y the vector of outputs calculated by the output layer, u the vector of inputs that excites the input layer and $\theta = \{w_1, b_1, w_2, b_2\}$ the network parameters (weights associated with node connections) that need to be estimated from data during the training process. The MLP expressed by Eq. (15) is of static nature. The extension to time series data is straightforward by considering time lagged inputs/outputs to the network. Box 5 illustrates such a dynamic MLP for the Park&Ramirez bioreactor problem. Kingma and Ba (2017) have shown how a deep MLP may be efficiently trained using the ADAM algorithm with (nodes) dropout. A network is considered deep when it has more than 2 hidden layers. This new development will likely boost new applications for bioreactor modeling and control in the near future (Salah and Fourati 2019).

Box 5. Dynamic Multilayer Perceptron Model for the Park and Ramirez (1988) bioreactor

A dynamic Multilayer Perceptron (MLP) model was trained on the dataset described in Box 1. The adopted MLP architecture is a standard 3-layered network (Eq. 20) with linear input/output layers and with a single tangent hyperbolic hidden layer (Fig. 5A). The output layer predicts the state in the future time instant $t+1$, $y(t+1) = [X(t+1), S(t+1, P_M(t+1), P_T(t+1), V(t+1)]^T$. The input nodes are the control inputs and state variables at the current time, t, and past time instants $t-1$ and $t-2$ $\{t,\ F(t),\ y(t), t-1, y(t-1), F(t-1), t-2, F(t-2), y(t-2)\}$. The training was performed in batch mode in the sense of weighted least squares:

$$WLS = \frac{1}{T}\sum_{i,t}\left(\frac{y_i(t)-y_{MLP,i(t)}}{\sigma_i}\right)^2, \quad (5.1),$$

with $y = [X, S, P_M, P_T, V]^T$ the measured state, y_{MLP} the predicted state, $T = 640$ the number of training patterns, and σ the standard deviation of the measurement error (Box 1). The cost function was minimized employing the Levenberg-Marquardt solver, with gradients calculated by error back-propagation. The training was repeated 10 times with initial random weights between -0.01 and 0.01. Cross-validation was applied using the data of cultivation runs 1-8 as training set whereas as the validation dataset comprised the same 1-8 cultivation runs with additional Gaussian error (to signalize the onset of noise modeling during the training). The final testing of the model was carried out using cultivation runs 9-16 as the test dataset. The number of input and hidden nodes were varied to ensure a final parsimonious model, whereas the number of output nodes was fixed to 5. The results of the training are shown in Figs. (5B,C). The training resulted in a final WLS of 0.15 and 2.59 for the training and validation sets respectively. All together the results suggests an accurate dynamic model in the training-validation domain (Fig 5B,C). The WLS of the test set was however 30.78, about 12fold higher than the validation WLS showing that the MLP prediction performance degraded considerably outside the training-validation domain. As stated in Box 1, the 16th cultivation run is the optimal fed-batch optimized by Park and Ramirez (1988). Cultivation 16 was included in the test dataset to assess the predictive power of the dynamic MLP at the optimal operating conditions. Fig. (5D-H) shows the state variables dynamic profiles for run 16 predicted by the dynamic MLP with respective 95% confidence bounds. Despite the higher test error, the final MLP model described fairly well the optimal reactor dynamics.

Figure 5. A – Dynamic MLP architecture for the Park and Ramirez (1988) bioreactor. Number of linear input nodes: 11; Number of $tanh$ hidden nodes: 5; Number of linear

output nodes: 5; Number of weights: 90. **B** - Modelling results for the validation dataset (640 points). The X-axis represents measured patterns, while the Y-axis represents MLP predictions. **C**- Modelling results of the validation dataset (640 points). The X-axis represents measured patterns, while the Y-axis represents MLP predictions. **D,E,F,H** – comparison of measured dynamic profile and MLP predicted dynamic profile for the optimal cultivation run 16: Biomass (**D**), Substrate (**E**), Total protein (**F**) and secreted protein (**H**). The colored intervals represent MLP predictions and respective 95% confidence intervals. The black dotted line represents the real profile described in Box 1. The symbols represent the training patterns with Gaussian error.

3.1.2 Decision trees (DT)

The DTs (DeLisle and Dixon 2004) is a simple case of a non-parametric supervised model and can represent any function of the input attributes, with the rules defined as a tree (consists of nodes and branches). The use of a training dataset defines the set of rules that will be sequentially employed to a new observation until a class is estimated. This process goes on until a leaf (terminal) node is satisfied, corresponding to the decision outcomes (i.e., continues or categorical value) or one stopping rules are reached. The rules for each node are given by the division of the dataset producing better discriminative ability. DTs are one of the most popular algorithms due to their high human interpretability and its simplicity to implement/use. In the context of bioreactor modeling, DTs can be applied, for example, to identify critical process parameters using information from different fermentation runs (Buck et al. 2002) and to find the combination of operating variables for algal biomass and lipid production (Cosgun et al. 2021). They have also been employed to optimize fermentation medium (Bapat and Wangikar 2004).

The relationship between the outcome (y) and features (x) is described by,

$$y = \sum_{m=1}^{M} c_m \, I\{x \in Rm\} \quad (21)$$

Here, each instance falls into exactly one leaf node (subset of R_m), c_m is the weight given to the m*th* transformation and $I_{\{x \in R_m\}}$ is the function that returns 1 if x is in the subset of R_m and 0 otherwise.

3.1.3 Random Forest (RF)

A RF (Breiman 2001) is an ensemble method that combines different DT, each with the same nodes. The RF algorithm has two main steps: (i) RF creation and (ii) make a prediction from the classifier created in step (i). This algorithm uses the sample bootstrapping aggregation method (Rindskopf 1997) for each DT. Additionally, a feature sampling is performed, making classifiers more robust to missing values and more uncorrelated to each other. For large number of trees, more accurate results are expected. This model prevents data overfitting and is simple to train. For a training set T = {(x_1, y_1). …, (x_n, y_n)} of N observations from random vectors (x, y), the developed RF will be an ensemble of k trees {$t_1(x)$. …, $t_k(x)$}. The ensemble produces k outputs {$y_1 = t_1(x)$,…, $y_k = t_k(x)$}, where y_k, k = {1,2, …., k} is the prediction for a classifier by the k*th* tree.

RF methods can be used as regression, classification and to assess feature importance, making it an algorithm with different applications on real-world problems. An example is given by Melcher, et al. (2015) who use RF technique to predict cell dry mass and recombinant protein based on online process parameters and spectroscopic information. Recently, RF have been employed for on-line fault diagnosis in a bioreactor operation (Shrivastava et al. 2017).

Box 4. Approaches associated with unsupervised learning for bioprocesses problems

K-means clustering is a heuristic unsupervised technique that creates partitions of similar characteristics in the same cluster (represented by *K*) and iteratively updates them (Yu et al. 2020). The number of clusters need to be specified in advance and each random data point (*x*) can only be assigned in one cluster center (centroid) based on feature similarity. The algorithm stops when the stopping criteria is obeyed (i.e., no data points assignment changes the clusters, or the sum of distances is minimized).

Mathematically, this algorithm iterates between two main steps:

i) Initialize randomly the cluster centroids $\{\mu_1, \mu_2, \mu_3, \ldots, \mu_k\} \in R^n$;

ii) Repeat until convergence for:

Each datapoint *i*, is set to its nearest centroid based on,

$$c^i = arg \ \ min_j \ dist \ \ |x^i - \mu_j|^2 \tag{6.1}$$

Each *j*, the centroids are recomputed by,

$$\mu_j = \frac{\sum_{i=1}^{m} 1\{c^i = j\} x^i}{\sum_{i=1}^{m} 1\{c^i = j\}} \tag{6.2}$$

The K-means clustering algorithm inputs are the datasets and the number of clusters *K*.

Dimensionality Reduction (DR) aims to reduce the number of features while preserving most of the relevant information or structure of the data (Butcher and Smith 2020). DR can be performed by two major approaches: feature selection and feature extraction/transformation. The feature selection is the process of choosing a subset of all features according for a given objective criteria (e.g., minimize the information loss or maximize class discrimination) and feature extraction of creating new features by combining existing ones. Feature selection differs from feature extraction where features

are non-linear combinations of all original features. The main feature selection techniques are the filters, embedded methods and wrappers models (Jovic et al. 2015). Another widely used dimensionality reduction technique in the bioprocess field is the principal component analysis (PCA). The goal of PCA is to explain the maximum variance of data in as few dimensions as possible. The main steps are:

i) Mean center the data;

ii) Compute the covariance matrix (scatter of data);

iii) Compute the eigenvectors (e_1,e_2, … , e_m) and eigenvalues ($\lambda_1 \geqslant \lambda_2 \geqslant \ldots, \geqslant \lambda_m \geqslant$) of the covariance matrix; the eigenvector with the k^{th} largest eigenvalue (λ_k) is the k^{th} principal component and the ratio $\sum_{j=1}^{k} \lambda_j^2 \; / \; \sum_{j=1}^{n} \lambda_j^2$ is the proportion of variance captured by k^{th} principal component.

iv) keep the large *k* eigenvalues (dimensionality reduction, $k \leqslant m$).

3.2 Hybrid mechanistic/ML bioreactor models

A very promising approach for bioreactor modeling is the combination of mechanistic models with ML into hybrid model structures. The combination of mechanistic models with ANNs for bioreactor dynamic modeling was first suggested by Psichogios and Ungar (1992) and Thompson and Kramer (1994). Thompson and Kramer (1994) classified this problem as a hybrid semiparametric modeling problem. Hybrid semiparametric models integrate parametric functions with fixed structure stemming from *prior* process knowledge (for example, macroscopic material balance equations) with nonparametric functions with loose structure that need to be identified from process data (for example a MLP as in the paper by Psichogios and Ungar (1992) or a radial basis function network, as in the paper by Thompson and Kramer (1994)). The main motivation was to cope with ANN disadvantages such as the inability to comply with process constraints, the tendency

for data overfitting, and the poor predictive power outside the training-validation domain. The advantages of hybrid modeling may be stated in *lato sensu* as a more efficient usage of knowledge for process modeling, which ultimately translates in more accurate, precise and robust process models (Schubert et al., 1994). Many other hybrid bioreactor modeling papers followed (e.g. Preusting et al., 1996, Andserson et al., 2000, Chen et al., 2000, Galvanauskas et al., 2004, Oliveira, 2004, Teixeira et al., 2007) reviewed by von Stosch et al. (2014). Here we focus on the general bioreactor hybrid model proposed by Oliveira (2004). This hybrid structure is formed by the general state-space macroscopic material balance Eqs. (2a,b).

$$\frac{dc}{dt} = r - Dc + Dc_{in} + q \tag{2a}$$

$$\frac{dV}{dt} = DV \tag{2b}$$

The reaction rates term, r, is defined as a flexible mixture of parametric and nonparametric functions with the following general form:

$$r = KH(c)\,\rho(c,\theta) \tag{22}$$

with K the yields matrix, $H(c)$ a set of known kinetic rate functions (with fixed structure and known parameters; for example Monod-type kinetics), and $\rho(c,\theta)$, a loose function with unknown structure that needs to be identified from data. The MLP network has been the preferred ML method in the context of the general bioreactor hybrid model.

$$\rho(c,\theta = \{w_1, b_1, w_2, b_2\}) = w_2\, tanh(w_1 c + b_1) + b_2 \tag{23}.$$

The main motivation for the general hybrid model structure is to provide a flexible framework to include all reliable mechanistic knowledge in the models and to decrease the dimensionality of the ML identification problem. It explicitly assumes that

macroscopic material balance equations are known *a priori* in most of the bioreactor modeling problems. The less understood part of the model in a mechanistic sense are the reaction kinetics. Thus, the experimental design and ML modeling should focus on the unknown parts, which are (some of) the reaction kinetics. In this way ML does not replace mechanistic models, it rather complements or improves existing mechanistic models. Box 6 illustrates the application of the general hybrid model concept to the Park and Ramirez (1988) bioreactor problem.

Box 7. General hybrid model for the Park&Ramirez bioreactor

The general bioreactor hybrid model (Eqs. 2ab, 22 and 23) was applied to the Park and Ramirez (1988) bioreactor. It is assumed that the material balance equations are known whereas the reaction kinetics are unknown. The ML identification is thus focused on the unknown reaction kinetics. The hybrid model structure is shown in Fig. (6A). The MLP has the same layer structure as in Box 5. The input nodes are the concentration of substrate at the current time, $\{S\}$. The output layer predicts the kinetic rates at the current time, $\{\Phi,\ f_P,\ \mu\}$. The material balances Eqs. (1.1-1.5) listed in Box 1 are connected in series with the MLP. The training of the hybrid model adopted here is comparable (but not the same due model structural differences) to the standalone MLP described in Box 5. The cost function was also the sum of weighted square errors,

$$WLS = \frac{1}{T}\sum_{i,t}\left(\frac{y_i(t)-y_{hyb,i}(t)}{\sigma_i}\right)^2, \qquad (7.1),$$

with $y = [X, S, P_T, P_M]^T$ the measured state, y_{hyb} the predicted state, $T = 512$ the number of training patterns (less than in Box 5 because volume is perfectly predicted by the hybrid model), and σ the standard deviation of the measurement error $\sigma = [0.25, 0.1, 0.1, 0.1]^T$. The Levenberg-Marquardt algorithm was the solver chosen as in Box 5, but with a major

difference in the calculation of gradients, which were computed by the sensitivities method (Oliveira, 2004). For the sake of comparability, the training was repeated 10 time with random initial weights between -0.01 and 0.01. Cross-validation was applied with the same data partitioning described in Box 5. The results of the training of the hybrid model are shown in Figs. (6B-E). The final training error was 1.60 and 2.24 for the training and validation partitions respectively. These values are comparable to those obtained with the standalone dynamic MLP of **b**ox 5. The main difference lies in the modeling error of the test dataset, which was 4.11 for the hybrid model, 7fold smaller than that for the standalone dynamic MLP. Fig. (6D-H) shows the state variables dynamic profiles for run 16 predicted by the hybrid model with respective 95% confidence bounds. All together these results suggest that the hybrid model has higher predictive power than the standalone dynamic MLP. Since the data was the same, and the training methods are comparable, the higher predictive power is attributed to structural advantages of the hybrid model.

Figure 6. A – Hybrid model structure for the Park and Ramirez (1988) bioreactor. Number of linear input nodes: 1; Number of $tanh$ hidden nodes: 3; Number of linear output nodes: 3; Number of weights: 18. **B** - Modelling results for the validation dataset (512 points). The X-axis represents measured patterns, while the Y-axis represents hybrid model predictions. **C**- Modelling results of the validation dataset (512 points). The X-axis represents measured patterns, while the Y-axis represents hybrid model predictions. **D,E,F,H** – comparison of measured dynamic profile and hybrid model predicted dynamic profile for the optimal cultivation run 16: Biomass (**D**), Substrate (**E**), Total protein (**F**) and secreted protein (**H**). The colored intervals represent MLP predictions and respective

95% confidence intervals. The black dotted line represents the real profile described in Box 1. The symbols represent the training patterns with Gaussian error.

---

4. Conclusions and future perspectives

Mathematical models are recognized as fundamental tools in chemical and biological engineering enabling to better understand process mechanisms, to reduce the experimental workload for process development, to increase the robustness of process operation, to improve productivity and yield, among many other potential benefits. While process systems engineering tools have proven determinant for the development and operation of chemical processes, the penetration in the bio-industries is lagging behind. A major bottleneck has been the poor understanding of biological reaction systems, stemming from its overwhelming complexity allied with the lack of analytical technologies to provide the required experimental evidence for the development of more detailed models. There is still today the perception that bioreactor models are more difficult to develop (higher costs) and less performing (lower benefits) in comparison to chemical reactor models. This apparently less attractive benefit/cost ratio has hampered the deployment of a consistent systems bioengineering toolbox in the bio-industries.

With the emergence of systems biology in the early 00s, several industrial cell lines have been sequenced and deeply investigated in their molecular biology traits and mechanisms. In particular, genome-scale models (GEMs) have been developed for the most important cell lines/microorganisms used in industry. While the development of GEMs for individual cell lines is work in progress, providing only a scaffold of the underlying biology, they offer the opportunity for holistic process modeling, linking cell line development, culture medium design, reactor optimization with downstream unit

operations. GEMs may guide the integration of the different scales thereby realizing the concept of holistic models for process platforms. The integration of GEMs in bioreactor macroscopic models faces however many challenges. Efficient and automatic reduction tools are needed to decrease the complexity of the model by taking into account process operation constraints such as the culture media composition, the feedings composition and other operating parameters. Also the removal of unnecessary reactions such as futile cycles, limitless ATP production, thermodynamically unfeasible pathways with unrealistic global yields. The reduction of the dynamical order is another major challenge in GEMs. Some intracellular processes exhibit monostable dynamical properties while others exhibit bistable behavior, which disrupt the dynamic behavior of the process. This complex intracellular dynamic behavior has been referred to by the unstructured modeling community as the "memory effect". A toolbox for the reduction of GEMs to reactor operation constraints will offer the opportunity to discriminate the critical dynamic processes to include in the bioreactor model for a reliable and parsimonious prediction of the process macroscopic state including the "memory effect".

Opposed to mechanistic modeling, data-driven modeling and ML are primarily focused on the predictive power with limited gain on process understating. The main bottleneck is the availability of thorough datasets covering the full domain of process operation. While ML in particular has enjoyed a tremendous development in the fields of image analysis and speech recognition, bioprocess applications are hindered by the scarcity of data in routine operation. The widespread use of high-throughput cultivation techniques linked with multi-data technologies will undeniably create novel opportunities for ML applications to bioprocesses. Such technologies generate large amounts of omics data, typically high-dimensional and sparse, which are difficult to integrate in bioreactor models. State-of-the-art algorithms of ML offer the tools to deal with some of the faced

challenges, by unraveling relationships and predictions from complex datasets without the need of *a priori* mechanistic knowledge. However, to accelerate more successful applications of data-driven approaches, high-quality bioprocess data repositories preferably in machine-readable format and new computational algorithms/tools to combine the benefits of ML and mechanistic information should be produced.

The apparently conflicting objectives between process understanding and predictive power may be mitigated by the adoption of hybrid modeling formalisms. Hybrid mechanistic/ML modeling has emerged in recent years as a promising technique for bioreactor modeling particularly in the biopharma sector. Hybrid modeling balances the advantages and disadvantages of both techniques. Many published studies have proven the superiority of hybrid mechanistic/ML model structures when benchmarked against the standalone mechanistic or ML model components. It tends to be less data dependent and more mechanistically trackable then standalone ML. It tends to be more predictive than standalone mechanistic models. Hybrid models combined with intensified statistical design of experiments have proven to substantially reduce the experimental workload for process development. There are however many challenges ahead in the hybrid modeling field. Hybrid modeling has been limited to relatively simple model structures and is difficult to scale to large problems, particularly to genome scale models. With current methods it is particularly difficult to develop hybrid models with detailed mechanistic modeling of intracellular phenomena. Novel model structures and training algorithms are needed particularly for large-scale hybrid models that integrate the different scales. The combination of symbolic and numeric computation frameworks will likely enable to scale-up hybrid models to more complex bioreactor problems with acceptable computation costs. The “hybridization” of GEMs and machine learning is particularly promising. Hybrid GEMs may guide the integration of the different stages of upstream

and downstream processing thereby realizing the concept of holistic models for process platforms. The embedded machine learning components will confer the learning through experience feature in the realm of Industry 4.0. From our point of view, solving these formidable challenges is just possible through inter- and multi-disciplinary collaborations between academia and industry.

5. References

Alpaydin, E. (2020) Introduction to machine learning, The MIT Press, Cambridge, Massachusetts.

Anderson, E. C., Bell, G. I., Petersen, D. F., & Tobey, R. A. (1969). Cell growth and division: IV. Determination of volume growth rate and division probability. Biophysical journal, 9(2), 246-263.

Anderson, J. S., McAvoy, T. J., & Hao, O. J. (2000). Use of hybrid models in wastewater systems. Industrial & Engineering Chemistry Research, 39(6), 1694-1704.

Andrews JF. A mathematical model for the continuous culture of microorganisms utilizing inhibitory substrates. Biotechnology and Bioengineering. 1968;10:707-723. DOI: 10.1002/bit.260100602

Ataai, M. M., & Shuler, M. L. (1985). Simulation of CFSTR through development of a mathematical model for anaerobic growth of Escherichia coli cell population. Biotechnology and bioengineering, 27(7), 1051-1055.

Back, T., (2000) Introduction to evolutionary algorithms in Evolutionary Computation 1: Basic Algorithms and Operators. CRC Press

Bailey, J.E. and Ollis, D.F. (1986). Biochemical Engineering Fundamentals. McGraw-Hill, New York, USA.

Baker Ruth E., Peña Jose-Maria, Jayamohan Jayaratnam and Jérusalem Antoine 2018 Mechanistic models versus machine learning, a fight worth fighting for the biological community? Biol. Lett.142017066020170660, http://doi.org/10.1098/rsbl.2017.0660

Banga, J., Moles, C., Alonso, A., Balsa-Canto, E. (2003). Dynamic Optimization Of Bioreactors: A Review. Proc. Indian Natl. Sci. Acad.. 69.

Bapat, P.M. and Wangikar, P.P. (2004) Optimization of Rifamycin B fermentation in shake flasks via a machine-learning-based approach. Biotechnology and Bioengineering 86(2), 201-208.

Bastin G, Dochain D (1990) On-line estimation and adaptive control of bioreactors. Elsevier, Amsterdam

Baughman, D.R. and Liu, Y.A. (1994) An Expert Network for Predictive Modeling and Optimal-Design of Extractive Bioseparations in Aqueous 2-Phase Systems. Industrial & Engineering Chemistry Research 33(11), 2668-2687.

Bellman, R. E. (2003). Dynamic Programming. Dover Publications, Inc., USA.

Blanch, H.W. and Clarck, D.S. (1996). Biochemical Engineering. Marcel Dekker, Inc. New York, USA.

Breiman, L. (2001) Random forests. Machine Learning 45(1), 5-32.

Breve, F.A. and Pedronette, D.C.G. (2016) Combined Unsupervised and Semi-Supervised Learning for Data Classification. 2016 Ieee 26th International Workshop on Machine Learning for Signal Processing (Mlsp).

Bryson, A.E., & Ho, Y.-C. (1975). Applied Optimal Control: Optimization, Estimation, and Control (1st ed.). CRC Press.

Buck, K.K.S., Subramanian, V. and Block, D.E. (2002) Identification of critical batch operating parameters in fed-batch recombinant E-Coli Fermentations using decision tree analysis. Biotechnology Progress 18(6), 1366-1376.

Butcher, B. and Smith, B.J. (2020) Feature Engineering and Selection: A Practical Approach for Predictive Models. American Statistician 74(3), 308-309.

Carrondo, Manuel J. T., Alves, Paula M.; Carinhas, N; Glassey, J; Hesse, F; Merten, OW; Micheletti, M; Noll, T; Oliveira, R; Reichl, U; Staby, A; Teixeira, AP; Weichert, H; Mandenius, CF, (2012) How can measurement, monitoring, modeling and control advance cell culture in industrial biotechnology? Biotechnology journal, 7(12), pp 1522-1529, doi: 10.1002/biot.201200226

Chen, L., Bernard, O., Bastin, G., & Angelov, P. (2000). Hybrid modelling of biotechnological processes using neural networks. Control Engineering Practice, 8(7), 821-827.

Cook, C.E., Bergman, M.T., Cochrane, G., Apweiler, R. and Birney, E. (2018) The European Bioinformatics Institute in 2017: data coordination and integration. Nucleic Acids Res 46(D1), D21-D29.

Cornish-Bowden, A. (1995). Metabolic control analysis in theory and practice. In Advances in molecular and cell biology (Vol. 11, pp. 21-64). Elsevier.

Cosgun, A., Gunay, M.E. and Yildirim, R. (2021) Exploring the critical factors of algal biomass and lipid production for renewable fuel production by machine learning. Renewable Energy 163, 1299-1317.

Costa RS, Machado D, Rocha I, Ferreira EC: Hybrid dynamic modeling of Escherichia coli central metabolic network combining Michaelis-Menten and approximate kinetic equations. Biosystems 2010, 100:150-157.

DeLisle, R.K. and Dixon, S.L. (2004) Induction of decision trees via evolutionary programming. Journal of chemical information and computer sciences 44(3), 862-870.

Delvigne, F., Zune, Q., Lara, A. R., Al-Soud, W., & Sørensen, S. J. (2014). Metabolic variability in bioprocessing: implications of microbial phenotypic heterogeneity. Trends in Biotechnology, 32(12), 608-616.

Dimassimo, C., Montague, G.A., Willis, M.J., Tham, M.T. and Morris, A.J. (1992) Towards Improved Penicillin Fermentation Via Artificial Neural Networks. Computers & Chemical Engineering 16(4), 283-291.

Dochain, D., Babary, J.P. and Tallmaamar, N. (1992) Modeling and Adaptive-Control of Nonlinear Distributed Parameter Bioreactors Via Orthogonal Collocation. Automatica 28(5), 873-883.

Domach, M. M., & Shuler, M. L. (1984). A finite representation model for an asynchronous culture of E. coli. Biotechnology and bioengineering, 26(8), 877-884.

Dorigo, M., Maniezzo, V., Colorni, A. (1996). Ant system: optimization by a colony of cooperating agents. IEEE Transac. Syst. Man Cyb. B, 26(1)

Fadda, S., Cincotti, A., & Cao, G. (2012). A novel population balance model to investigate the kinetics of in vitro cell proliferation: part I. Model development. Biotechnology and bioengineering, 109(3), 772-781.

Forster J, Famili I, Fu P, Palsson BO, Nielsen J (2003) Genome-scale reconstruction of the Saccharomyces cerevisiae metabolic network. Genome Res 13(2):244–253. https://doi.org/10.1101/gr.234503

Galvanauskas, V., Simutis, R., & Lübbert, A. (2004). Hybrid process models for process optimisation, monitoring and control. Bioprocess and Biosystems Engineering, 26(6), 393-400.

Ganusov, V. V., Bril'kov, A. V., & Pechurkin, N. S. (2000). Mathematical modeling of population dynamics of unstable plasmid-containing bacteria during continuous cultivation in a chemostat. Biofizika, 45(5), 908-914.

Han K, Levenspiel O. Extended monod kinetics for substrate, product, and cell inhibition. Biotechnology and Bioengineering. 1988;32:430-447. DOI: 10.1002/bit.260320404

Haykin, S.S. (2009) Neural networks and learning machines, Prentice Hall, New York.

Hefzi, H., Ang, K. S., Hanscho, M., Bordbar, A., Ruckerbauer, D., Lakshmanan, M., ... & Lewis, N. E. (2016). A consensus genome-scale reconstruction of Chinese hamster ovary cell metabolism. Cell Systems, 3(5), 434-443.

Henson, M. A. (2003). Dynamic modeling and control of yeast cell populations in continuous biochemical reactors. Computers & Chemical Engineering, 27(8-9), 1185-1199.

Hjortso, M. A., & Nielsen, J. (1995). Population balance models of autonomous microbial oscillations. Journal of biotechnology, 42(3), 255-269.

Holland, J., (1975) Adaptation in natural and artificial systems : an introductory analysis with applications to biology, control, and artificial intelligence. University of Michigan Press Ann Arbor

Hoskins, J.C. and Himmelblau, D.M. (1992) Process-Control Via Artificial Neural Networks and Reinforcement Learning. Computers & Chemical Engineering 16(4), 241-251.

Jens Smiatek, Alexander Jung, Erich Bluhmki, (2020) Towards a Digital Bioprocess Replica: Computational Approaches in Biopharmaceutical Development and Manufacturing, Trends in Biotechnology, Volume 38, Issue 10, 2020, Pages 1141-1153, https://doi.org/10.1016/j.tibtech.2020.05.008.

Jordan, M.I. and Mitchell, T.M. (2015) Machine learning: Trends, perspectives, and prospects. Science 349(6245), 255-260.

Joseph, B. and Hanratty, F.W. (1993) Predictive Control of Quality in a Batch Manufacturing Process Using Artificial Neural-Network Models. Industrial & Engineering Chemistry Research 32(9), 1951-1961.

Jovic, A., Brkic, K. and Bogunovic, N. (2015) A review of feature selection methods with applications. 2015 8th International Convention on Information and Communication Technology, Electronics and Microelectronics (Mipro), 1200-1205.

Kennedy, J., Eberhart, R. (1995). Particle Swarm Optimization. Proceedings of IEEE International Conference on Neural Networks, 4

Kingma, D. P., & Ba, J. (2014). Adam: A method for stochastic optimization. arXiv preprint arXiv:1412.6980.

Kirkpatrick, S., Gelatt Jr, C., Vecchi, M., (1983). Optimization by Simulated Annealing. Science. 220

Krogh, A. (2008) What are artificial neural networks? Nature Biotechnology 26(2), 195-197.

Larochelle, H., Bengio, Y., Louradour, J. and Lamblin, P. (2009) Exploring Strategies for Training Deep Neural Networks. Journal of Machine Learning Research 10, 1-40.

Larranaga, P., Calvo, B., Santana, R., Bielza, C., Galdiano, J., Inza, I., Lozano, J.A., Armananzas, R., Santafe, G., Perez, A. and Robles, V. (2006) Machine learning in bioinformatics. Brief Bioinform 7(1), 86-112.

Lee, J.H., Shin, J. and Realff, M.J. (2018) Machine learning: Overview of the recent progresses and implications for the process systems engineering field. Computers & Chemical Engineering 114, 111-121.

Liebermeister, W., & Klipp, E. (2006). Bringing metabolic networks to life: convenience rate law and thermodynamic constraints. Theoretical Biology and Medical Modelling, 3(1), 1-13.

Liebermeister, W., Uhlendorf, J., & Klipp, E. (2010). Modular rate laws for enzymatic reactions: thermodynamics, elasticities and implementation. Bioinformatics, 26(12), 1528-1534.

Liu, W. K., Li, S., & Belytschko, T. (1997). Moving least-square reproducing kernel methods (I) methodology and convergence. Computer methods in applied mechanics and engineering, 143(1-2), 113-154.

Luedeking, R., & Piret, E. L. (1959). A kinetic study of the lactic acid fermentation. Batch process at controlled pH. Journal of Biochemical and Microbiological Technology and Engineering, 1(4), 393-412.

Luus, R. (1992). On the Application of Iterative Dynamic Programming to Singular Optimal Control Problems, IEEE Trans. Autom. Control, 37(11)

Ma, Y., Norena-Caro, D.A., Adams, A.J., Brentzel, T.B., Romagnoli, J.A. and Benton, M.G. (2020) Machine-learning-based simulation and fed-batch control of cyanobacterial-phycocyanin production in Plectonema by artificial neural network and deep reinforcement learning. Computers & Chemical Engineering 142.

Mahadevan, R., Edwards, J. S., & Doyle III, F. J. (2002). Dynamic flux balance analysis of diauxic growth in Escherichia coli. Biophysical journal, 83(3), 1331-1340.

Mandenius, CF. Recent developments in the monitoring, modeling and control of biological production systems. Bioprocess Biosyst Eng 26, 347–351 (2004). https://doi.org/10.1007/s00449-004-0383-z

Mantzaris, N. V., Daoutidis, P., & Srienc, F. (2001). Numerical solution of multi-variable cell population balance models: I. Finite difference methods. Computers & Chemical Engineering, 25(11-12), 1411-1440.

Melcher, M., Scharl, T., Spangl, B., Luchner, M., Cserjan, M., Bayer, K., Leisch, F. and Striedner, G. (2015) The potential of random forest and neural networks for biomass and recombinant protein modeling in Escherichia coli fed-batch fermentations. Biotechnology Journal 10(11), 1770-1782.

McLamore, E.S., Huffaker, R., Shupler, M., Ward, K., Datta. S., Banks, M., Casaburi, G., Babilonia, J. and Foster, J., Digital Proxy of a Bio-Reactor (DIYBOT) combines

sensor data and data analytics to improve greywater treatment and wastewater management systems. Sci Rep 10, 8015 (2020). https://doi.org/10.1038/s41598-020-6478

Monk, J. M., Charusanti, P., Aziz, R. K., Lerman, J. A., Premyodhin, N., Orth, J. D., ... & Palsson, B. Ø. (2013). Genome-scale metabolic reconstructions of multiple Escherichia coli strains highlight strain-specific adaptations to nutritional environments. Proceedings of the National Academy of Sciences, 110(50), 20338-20343.

Monod J. The growth of bacterial cultures. Annual Review of Microbiology. 1949;3:371-394. DOI: 10.1146/annurev.mi.03.100149.0021037

Moser A., Appl C., Brüning S., Hass V.C. (2020) Mechanistic Mathematical Models as a Basis for Digital Twins. In: . Advances in Biochemical Engineering/Biotechnology. Springer, Berlin, Heidelberg. https://doi.org/10.1007/10_2020_152

Nargund, S, Guenther, K., and Mauch, K. The Move toward Biopharma 4.0. Genetic Engineering & Biotechnology News (2019) 53-55.http://doi.org/10.1089/gen.39.06.18

Nian, R., Liu, J.F. and Huang, B. (2020) A review On reinforcement learning: Introduction and applications in industrial process control. Computers & Chemical Engineering 139.

Nielsen, J., & Villadsen, J. (1994). Population Balances Based on Cell Number. In Bioreaction Engineering Principles (pp. 271-294). Springer, Boston, MA.

Nishimura, Y., & Bailey, J. E. (1981). Bacterial population dynamics in batch and continuous-flow microbial reactors. AIChE Journal, 27(1), 73-81.

Nocedal, J., Wright, S. (1999). Numerical Optimization. New York: Springer

Oliveira, R. (2004). Combining first principles modelling and artificial neural networks: a general framework. Computers & Chemical Engineering, 28(5), 755-766.

Palsson.B.O. (2002) In silico biology through "omics". Nature Biotechnology 20, 649-650.

Park, S., & Fred Ramirez, W. (1988). Optimal production of secreted protein in fed-batch reactors. AIChE Journal, 34(9), 1550-1558.

Pedregosa, F., Varoquaux, G., Gramfort, A., Michel, V., Thirion, B., Grisel, O., Blondel, M., Prettenhofer, P., Weiss, R., Dubourg, V., Vanderplas, J., Passos, A., Cournapeau, D., Brucher, M., Perrot, M. and Duchesnay, E. (2011) Scikit-learn: Machine Learning in Python. Journal of Machine Learning Research 12, 2825-2830.

Pigou, M., Morchain, J., Fede, P., Penet, M. I., & Laronze, G. (2017). An assessment of methods of moments for the simulation of population dynamics in large-scale bioreactors. Chemical Engineering Science, 171, 218-232.

Powell, B.K.M., Machalek, D. and Quah, T. (2020) Real-time optimization using reinforcement learning. Computers & Chemical Engineering 143.

Preusting, H., Noordover, J., Simutis, R., & Lübbert, A. (1996). The use of hybrid modelling for the optimization of the penicillin fermentation process. CHIMIA International Journal for Chemistry, 50(9), 416-417.

Psichogios, D. C., & Ungar, L. H. (1992). A hybrid neural network-first principles approach to process modeling. AIChE Journal, 38(10), 1499-1511.

Qin, Y.M., Yalamanchili, H.K., Qin, J., Yan, B. and Wang, J.W. (2015) The Current Status and Challenges in Computational Analysis of Genomic Big Data. Big Data Research 2(1), 12-18.

Quek, L. E., Dietmair, S., Hanscho, M., Martínez, V. S., Borth, N., & Nielsen, L. K. (2014). Reducing Recon 2 for steady-state flux analysis of HEK cell culture. Journal of biotechnology, 184, 172-178.

Rindskopf, D. (1997) An introduction to the bootstrap - Efron,B, Tibshirani,RJ. Journal of Educational and Behavioral Statistics 22(2), 245-245.

Rumelhart, D. E., Hinton, G. E., & Williams, R. J. (1986). Learning representations by back-propagating errors. nature, 323(6088), 533-536.

Salah, L.B. and Fourati, F. (2019) Deep MLP neural network control of bioreactor. 2019 10th International Renewable Energy Congress (Irec).

Savageau, M. A. (1970). Biochemical systems analysis: III. Dynamic solutions using a power-law approximation. Journal of theoretical biology, 26(2), 215-226.

Schubert, J., Simutis, R., Dors, M., Havlík, I., & Lübbert, A. (1994). Hybrid modelling of yeast production processes–combination of a priori knowledge on different levels of sophistication. Chemical Engineering & Technology: Industrial Chemistry-Plant Equipment-Process Engineering-Biotechnology, 17(1), 10-20.

Shin, J., Badgwell, T.A., Liu, K.H. and Lee, J.H. (2019) Reinforcement Learning - Overview of recent progress and implications for process control. Computers & Chemical Engineering 127, 282-294.

Shrivastava, R., Mahalingam, H. and Dutta, N.N. (2017) Application and Evaluation of Random Forest Classifier Technique for Fault Detection in Bioreactor Operation. Chemical Engineering Communications 204(5), 591-598.

Sidoli, F. R., Mantalaris, A., & Asprey, S. P. (2004). Modelling of mammalian cells and cell culture processes. Cytotechnology, 44(1), 27-46.

Singh, A., Thakur, N. and Sharma, A. (2016) A Review of Supervised Machine Learning Algorithms. Proceedings of the 10th Indiacom - 2016 3rd International Conference on Computing for Sustainable Global Development, 1310-1315.

Singh, M., Singh, R., Singh, S., Walker, G., & Matsoukas, T. (2020). Discrete finite volume approach for multidimensional agglomeration population balance equation on unstructured grid. Powder Technology, 376, 229-240.

Sohn, S. B., Graf, A. B., Kim, T. Y., Gasser, B., Maurer, M., Ferrer, P., ... & Lee, S. Y. (2010). Genome-scale metabolic model of methylotrophic yeast Pichia pastoris and its use for in silico analysis of heterologous protein production. Biotechnology journal, 5(7), 705-715.

Stanford, N. J., Lubitz, T., Smallbone, K., Klipp, E., Mendes, P., & Liebermeister, W. (2013). Systematic construction of kinetic models from genome-scale metabolic networks. PloS one, 8(11), e79195.

Storn, R., Price, K. (1997) Differential Evolution - a Simple and Efficient Heuristic for Global Optimization over Continuous Spaces, Journal of Global Optimization, 11, 341 - 359.

Sutton, R.S. and Barto, A.G. (1998) Reinforcement learning : an introduction, MIT Press, Cambridge, Mass.

Teixeira AP, Alves C, Alves PM et al. (2007) Hybrid elementary flux analysis/nonparametric modeling: application for bioprocess control. BMC Bioinformatics 8:30

Thiele, I., Swainston, N., Fleming, R. M., Hoppe, A., Sahoo, S., Aurich, M. K., ... & Palsson, B. Ø. (2013). A community-driven global reconstruction of human metabolism. Nature biotechnology, 31(5), 419-425.

Thompson, M. L., & Kramer, M. A. (1994). Modeling chemical processes using prior knowledge and neural networks. AIChE Journal, 40(8), 1328-1340.

Visser, D., & Heijnen, J. J. (2003). Dynamic simulation and metabolic re-design of a branched pathway using linlog kinetics. Metabolic engineering, 5(3), 164-176.

Von Stosch, M., Oliveira, R., Peres, J., & de Azevedo, S. F. (2014). Hybrid semi-parametric modeling in process systems engineering: Past, present and future. Computers & Chemical Engineering, 60, 86-101.

Wales, D. J., & Doye, J. P. (1997). Global optimization by basin-hopping and the lowest energy structures of Lennard-Jones clusters containing up to 110 atoms. The Journal of Physical Chemistry A, 101(28), 5111-5116.

Wolpert, D., Macready, W. (1997). No Free Lunch Theorems for Optimization, IEEE Transac. Evolut. Comp., 1

Xiang, Y., Gubian, S., Suomela, B., Hoeng, J. (2013) Generalized Simulated Annealing for Efficient Global Optimization: the GenSA Package for R. The R Journal, Volume 5/1

Yu, H., Wen, G.Q., Gan, J.Z., Zheng, W. and Lei, C. (2020) Self -paced Learning for K -means Clustering Algorithm. Pattern Recognition Letters 132, 69-75.

Zhu, G. Y., Zamamiri, A., Henson, M. A., & Hjortsø, M. A. (2000). Model predictive control of continuous yeast bioreactors using cell population balance models. Chemical Engineering Science, 55(24), 6155-6167.

Figure captions

Figure 1. The multiscale nature of a bioreactor system.

Figure 2. Simulation of 16 cultivation runs with the Park and Ramirez (1988) model eqs. (1.1-1.7). Numerical integration proceeded with a Runge-Kutta $4^{th}/5^{th}$ order solver. Small points refer to the simulation of 15 runs with 3 levels of constant feeding rate designed by central composite design with 3 factors, each factor representing a constant feeding rate in a 5-hour interval. The larger points represent the Park&Ramirez optimal control solution with maximal productivity of 32.4 g of secreted in the end of the culture.

Figure 3. Dynamic optimization for the Park and Ramirez (1988) bioreactor problem. A – Direct dynamic optimization with control vector parameterization schematic representation. B - Comparison of cumulative percentage undersize for different optimization methods run 10 times with a maximum limit of 50000 function evaluations with 10 discretization intervals. C – Optimal feeding profile and reactor volume obtained with the *differential evolution* method with 40 discretization intervals. D - Optimal biomass and substrate profiles obtained with the *differential evolution* method with 40

discretization intervals. E - Optimal total and secreted protein profiles obtained with the *differential evolution* method with 40 discretization intervals.

Figure 4. Workflow for typical supervised machine learning algorithms**.**

Figure 5. A – Dynamic MLP architecture for the Park and Ramirez (1988) bioreactor. Number of linear input nodes: 11; Number of $tanh$ hidden nodes: 5; Number of linear output nodes: 5; Number of weights: 90. **B -** Modelling results for the validation dataset (640 points). The X-axis represents measured patterns, while the Y-axis represents MLP predictions. **C**- Modelling results of the validation dataset (640 points). The X-axis represents measured patterns, while the Y-axis represents MLP predictions. **D,E,F,H** – comparison of measured dynamic profile and MLP predicted dynamic profile for the optimal cultivation run 16: Biomass (**D**), Substrate (**E**), Total protein (**F**) and secreted protein (**H**). The colored intervals represent MLP predictions and respective 95% confidence intervals. The black dotted line represents the real profile described in Box 1. The symbols represent the training patterns with Gaussian error.

Figure 6. A – Hybrid model structure for the Park and Ramirez (1988) bioreactor. Number of linear input nodes: 1; Number of $tanh$ hidden nodes: 3; Number of linear output nodes: 3; Number of weights: 18. **B -** Modelling results for the validation dataset (512 points). The X-axis represents measured patterns, while the Y-axis represents hybrid model predictions. **C**- Modelling results of the validation dataset (512 points). The X-axis represents measured patterns, while the Y-axis represents hybrid model predictions. **D,E,F,H** – comparison of measured dynamic profile and hybrid model predicted dynamic profile for the optimal cultivation run 16: Biomass (**D**), Substrate (**E**), Total protein (**F**) and secreted protein (**H**). The colored intervals represent MLP predictions and respective

95% confidence intervals. The black dotted line represents the real profile described in Box 1. The symbols represent the training patterns with Gaussian error.

List of figures

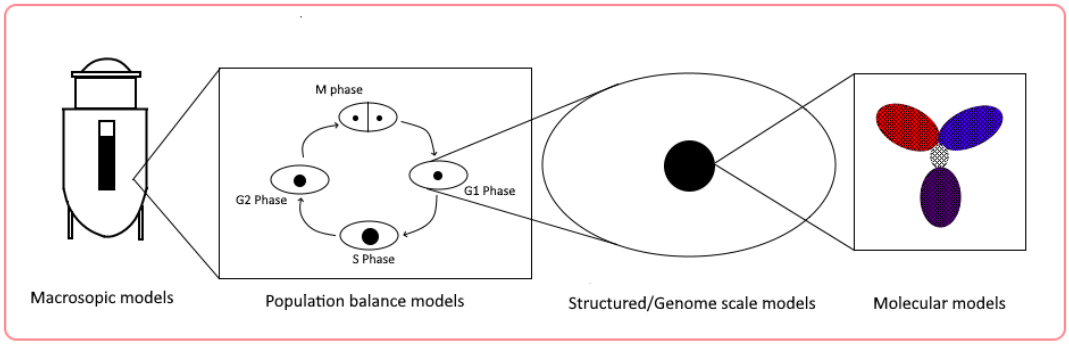

Figure 1

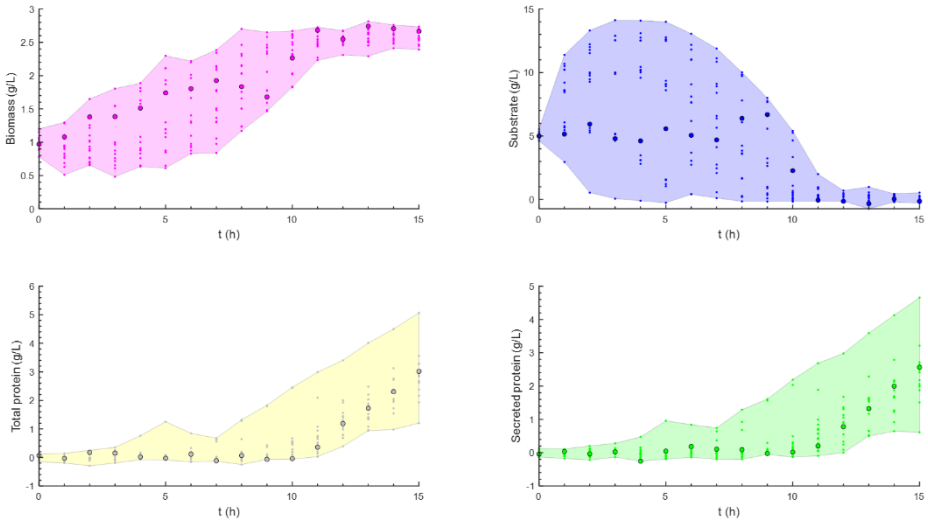
Biomass (g/L)
t (h)
Substrate (g/L)
t (h)
Total protein (g/L)
t (h)
Secreted protein (g/L)
t (h)

Figure 2

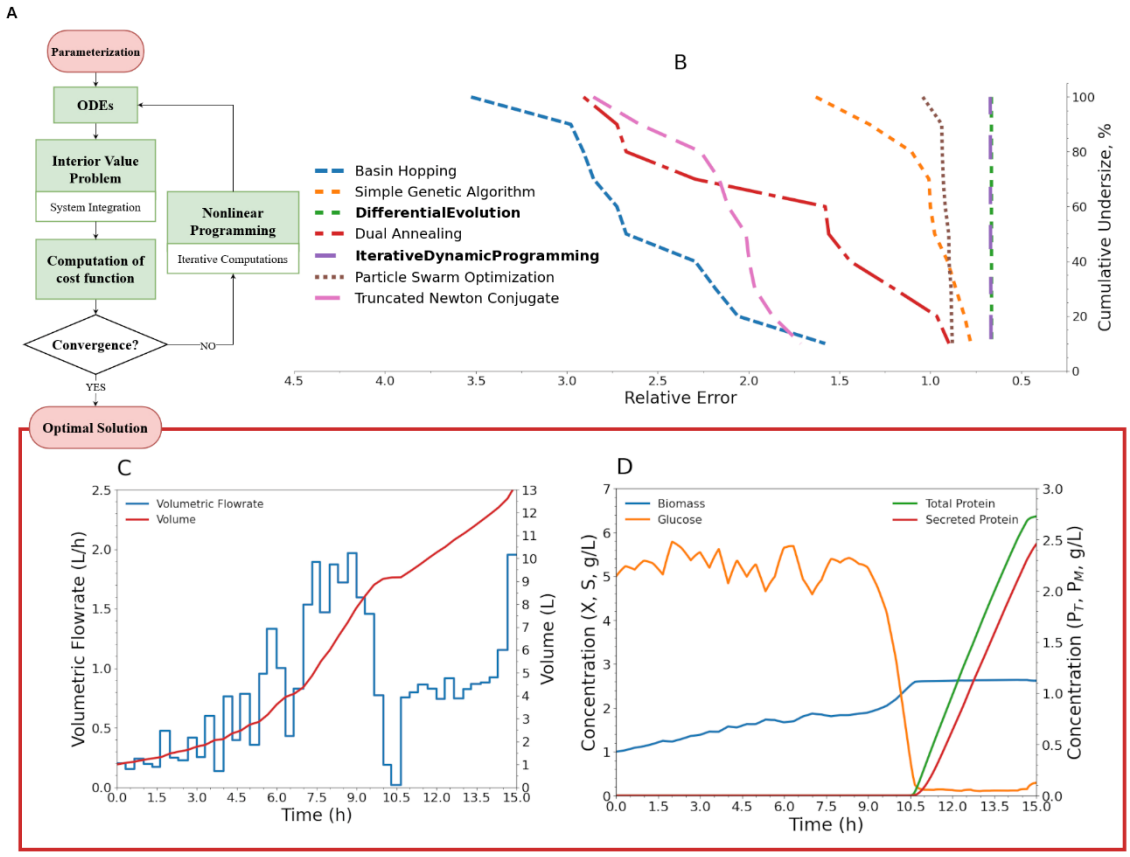
A
Parameterization
ODEs
Interior Value Problem
System Integration
Computation of cost function
Convergence?
NO
YES
Nonlinear Programming
Iterative Computations
Optimal Solution
B
Basin Hopping
Simple Genetic Algorithm
DifferentialEvolution
Dual Annealing
IterativeDynamicProgramming
Particle Swarm Optimization
Truncated Newton Conjugate
Relative Error
Cumulative Undersize, %
C
Volumetric Flowrate
Volume
Volumetric Flowrate (L/h)
Volume (L)
Time (h)
D
Biomass
Glucose
Total Protein
Secreted Protein
Concentration (X, S, g/L)
Concentration (P_T, P_M, g/L)
Time (h)

Figure 3

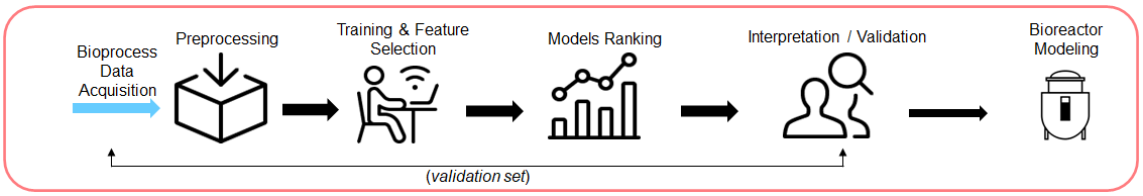
Bioprocess Data Acquisition
Preprocessing
Training & Feature Selection
Models Ranking
Interpretation / Validation
Bioreactor Modeling
(validation set)

Figure 4

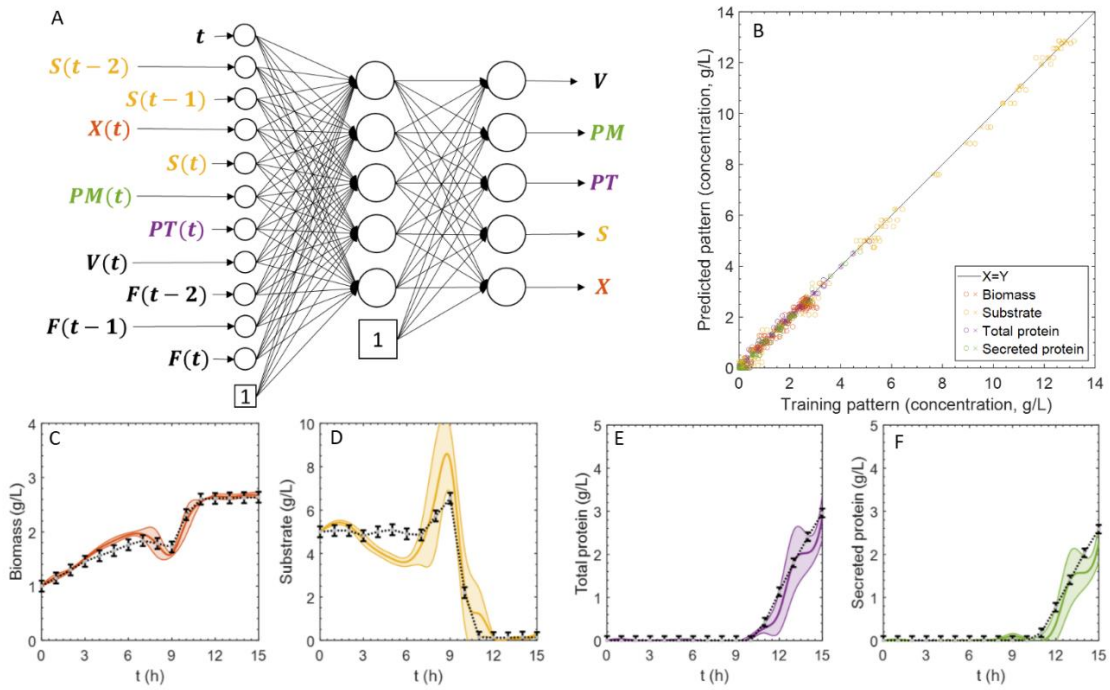
A
t
S(t − 2)
S(t − 1)
X(t)
S(t)
PM(t)
PT(t)
V(t)
F(t − 2)
F(t − 1)
F(t)
1
1
V
PM
PT
S
X
B
Predicted pattern (concentration, g/L)
Training pattern (concentration, g/L)
X=Y
Biomass
Substrate
Total protein
Secreted protein
C
Biomass (g/L)
t (h)
D
Substrate (g/L)
t (h)
E
Total protein (g/L)
t (h)
F
Secreted protein (g/L)
t (h)

Figure 5

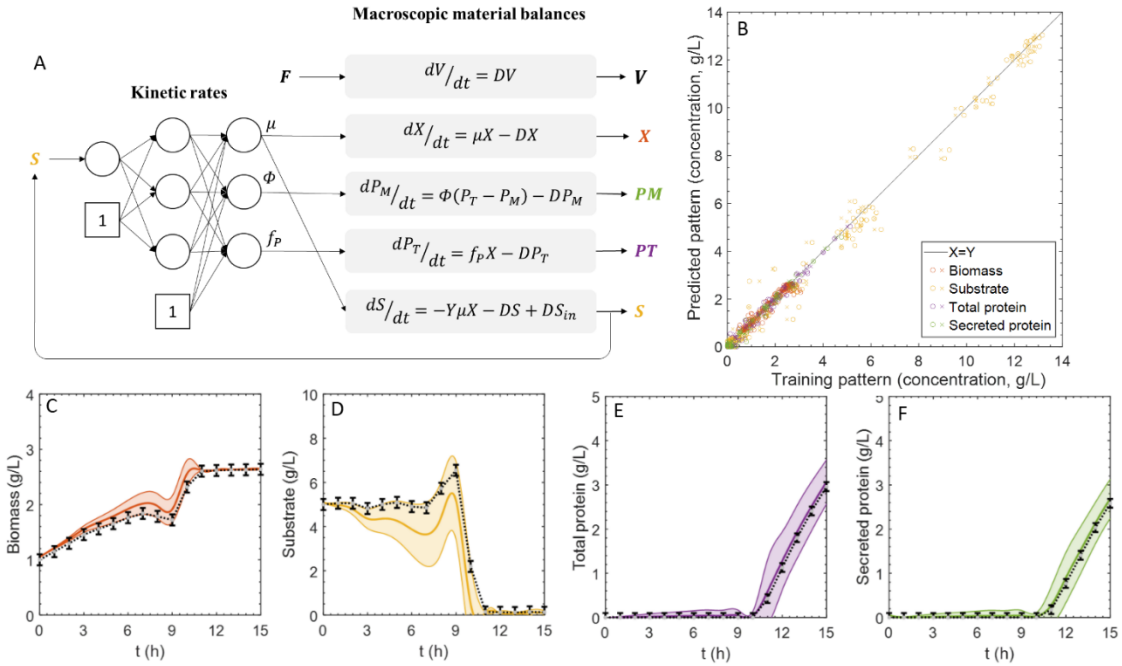
A
Macroscopic material balances
Kinetic rates
F
V
X
PM
PT
S
1
1
B
Predicted pattern (concentration, g/L)
Training pattern (concentration, g/L)
X=Y
Biomass
Substrate
Total protein
Secreted protein
C
Biomass (g/L)
t (h)
D
Substrate (g/L)
t (h)
E
Total protein (g/L)
t (h)
F
Secreted protein (g/L)
t (h)

Figure 6